C. R. Chimie 13 (2010) 494–501

Contents lists available at ScienceDirect

Comptes Rendus Chimie

www.sciencedirect.com

Full paper/Mémoire

Co–Mg–Al oxides issued of hydrotalcite precursors for total oxidation of volatile organic compounds. Identification and toxicological impact of the by-products

Cédric Gennequin [a,b], Serge Kouassi [a,b], Lucette Tidahy [a,b], Renaud Cousin [a,b], Jean-François Lamonier [a,1], Guillaume Garcon [a,b], Pirouz Shirali [a,b], Fabrice Cazier [a,c], Antoine Aboukaïs [a,b], Stéphane Siffert [a,b,*]

[a] Université Lille Nord de France, 59000 Lille, France
[b] ULCO, UCEIV, MREI, 59140 Dunkerque, France
[c] ULCO, CCM, MREI, 59140 Dunkerque, France

ARTICLE INFO

Article history:
Received 20 May 2009
Accepted after revision 11 January 2010
Available online 1 March 2010

Keywords:
VOC
Catalytic oxidation
Co-Mg-Al catalysts
Hydrotalcite
Lung toxicity
L132 cells
Toluene
Benzene
Cytotoxicity tests

ABSTRACT

Catalysts based on Co-Mg-Al, which were used for the total oxidation of toluene, were synthesized by using the hydrotalcite pathway. The calcination allowed us to obtain various mixed oxide types (i.e. Co_3O_4, Co_2AlO_4 or $CoAl_2O_4$), presenting mesopores of about 8 nm and high specific surface areas. The solids were tested for the total oxidation of toluene and showed a total selectivity in CO_2 and H_2O for 100% of toluene conversion. However, studies using diffuse reflectance infrared "operando" and GC-MS allowed us to identify intermediary by-products stemming from the catalytic oxidation of toluene: benzene and small quantities of benzaldehyde, styrene and acetophenone. In order to contribute to the improvement of the current scientific knowledge on volatile organic compound (VOC) toxicity in humans, the lung toxicity of toluene, benzene or their association was determined by using a human epithelial lung cell model (i.e. L132 cell line). VOC cytotoxicity was studied with three complementary methods: the enzymatic activity of extracellular lactate dehydrogenase (LDH), the enzymatic activity of mitochondrial dehydrogenase (mDH), and the incorporation of 5-Bromodesoxyuridine (5-BrdU). Taken together, these results showed the occurrence of adverse effects, notably reported by significant increases in LDH activity in cell culture supernatants, 24 hours after L132 cell exposure not only to toluene alone or benzene alone, but also to their association. This original approach allowed us to integrate some toxicological parameters to help the choice of new-dedicated catalysts for the oxidative conversion of VOC.

Mots clés :
COV
Oxydation catalytique
Catalyseurs à base de Co-Mg-Al
Voie hydrotalcite

RÉSUMÉ

Des catalyseurs à base de Co-Mg-Al destinés à l'oxydation totale du toluène ont été synthétisés en utilisant la voie hydrotalcite. La calcination à 500 °C a permis d'obtenir différents oxydes mixtes de type spinelles Co_3O_4, Co_2AlO_4 ou $CoAl_2O_4$ présentant des mésopores d'environ 8 nm et de grandes surfaces spécifiques. Les solides ont été testés dans l'oxydation totale du toluène et ont montré une sélectivité totale en CO_2 et H_2O pour

* Corresponding author. Université du Littoral-Côte d'Opale, Unité de Chimie Environnementale et Intéractions sur le Vivant, 145, avenue Maurice Schumann, 59140 Dunkerque, France.
E-mail address: siffert@univ-littoral.fr (S. Siffert).
[1] USTL, UCCS, UMR CNRS 8181, 59650 Villeneuve d'Ascq, France.

1631-0748/$ – see front matter
doi:10.1016/j.crci.2010.01.001

Toxicité pulmonaire
Cellules L132
Toluène
Benzène
Tests de cytotoxicité

100 % de conversion en toluène. Mais, des études par infrarouge en réflexion diffuse « operando » et par CPG-SM ont permis d'identifier les produits intermédiaires issus de l'oxydation catalytique du toluène : benzène et faibles quantités de benzaldéhyde, de styrène et d'acétophénone. Afin de mieux évaluer la toxicité de ces composés organiques volatils (COV) et de leurs sous-produits sur l'homme, la toxicité pulmonaire du toluène et du benzène a été étudiée non seulement pour les deux composés seuls mais aussi pour leur association, afin d'observer leur éventuelle interaction. Un modèle de cellules embryonnaires isolées à partir d'épithélium pulmonaire humain (lignée L132) a été exposé pendant six à 72 heures à des concentrations croissantes de toluène, de benzène ou de leur association. La cytotoxicité du (ou des) COV a été déterminée par trois méthodes complémentaires : l'activité enzymatique de la lactate déshydrogénase (LDH) extracellulaire, l'activité enzymatique de la déshydrogénase mitochondriale (DHm), et l'incorporation de la 5-Bromo-désoxyuridine (5-BrdU). Nos résultats ont suggéré des effets cytotoxiques, dès 24 heures, relativement faibles suite à l'exposition des cellules à chacun des COV, mais plus marqués suite à l'exposition à leur association. Cette approche originale permet l'intégration des paramètres de toxicité dans le choix de nouveaux catalyseurs dédiés à la conversion catalytique de COV.

1. Introduction

Volatile organic compounds (VOC) are pollutants because, in addition of being sometimes malodorous or toxic, they contribute to ozone formation [1]. In order to achieve the VOC abatement objectives, different techniques such as absorption, catalytic oxidation and thermal incineration for the VOC removal can be used. Catalytic oxidation is a promising process for VOC elimination, since the reaction operates at temperatures much lower than those required for thermal incineration. Moreover, catalytic deep oxidation is more selective and as it requires less heating, is more cost effective than direct combustion, when the VOC concentration is lower than 10,000 ppm. Manganese or cobalt oxides are the most active phases for catalytic oxidation of VOC [2–4] but these oxides usually present low specific area and poor thermal stability. An interesting way to obtain mixed oxide catalysts is through the use of hydrotalcites (HTs) or layered double hydroxides (LDHs) as precursors. Indeed, after calcination treatment mixed oxides are formed and possess unique properties like high surface area, good thermal stability, good mixed oxide homogeneity, and basic properties [5]. The structure of hydrotalcites can be derived from a brucite structure ($Mg(OH)_2$) [5] in which a part of the Mg^{2+} cations is substituted by a trivalent metal like Al^{3+}. The partial or the total substitution of Mg^{2+} and Al^{3+} is possible by divalent cations ($M^{2+} = Zn^{2+}$, Ni^{2+}, Cu^{2+}, Co^{2+}, etc.) and trivalent cations ($M^{3+} = Fe^{3+}$, Cr^{3+}, etc.), respectively. The positive charge of the metal hydroxide layers is compensated by interstitial layers built of anions ($A^{m-} = CO_3^{2-}$, NO_3^-, etc.) and water molecules. These materials gain increasing importance as catalyst precursors for many reactions of industrial interest [6] like CH_4 and methanol reforming [7,8], VOC oxidation [9,10], hydrodesulfurization of FCC gasoline [11], NO reduction [12] and removal of SO_2 and NOx [13]. In the present study, Co-Mg-Al hydrotalcites as precursors have been investigated for toluene oxidation catalysts. In order to evaluate the pertinence for using such precursors, conventional preparation of mixed oxides has also been performed. The catalytic oxidation of VOCs over metal oxides involves a complex process showing a variety of products under different conditions. In the present study, FTIR operando technique and sorbent tubes have been used for characterized VOC intermediate products.

Certainly, the reduction of VOC emissions is required in terms of public health, and, in this context, the catalytic treatment is an interesting solution to the oxidative degradation of VOC (i.e. toluene) into less toxic by-products (e.g. CO_2, H_2O) [14]. However, in the case of an incomplete catalysis, driven by non-optimal conditions (e.g. temperature) or by inactivation of the catalyst (e.g. aging, poisoning), toxic by-products can be formed during the catalysis treatment. Indeed, it has already been well established that the oxidative degradation of a VOC does not lead directly to the formation of CO_2 and H_2O, but through changes in complex cascades of chemical reactions. This has been well described in the case of toluene: the incomplete catalysis of its oxidative degradation induces the formation of toxic by-products such as benzyl alcohol, benzaldehyde and benzene. Hence, in this work, the cytotoxicity of toluene and/or one of its toxic by-products, benzene, have been carried out in an in vitro human lung target cell model (i.e. L132 cell line) through the determination of lactate dehydrogenase (LDH) activity in cell-free culture supernatants, on the one hand, and the determination of the mitochondrial dehydrogenase (MDH) activity and the incorporation of 5-Bromo-2-deoxyuridine (BrdU) in cultured cells, on the other hand.

2. Materials and methods

2.1. Preparation of hydrotalcites, hydroxides and corresponding calcined samples

A solution containing appropriate quantities of $Co(NO_3)_2.6H_2O$ (FLUKA), $Mg(NO_3)_2.4H_2O$ (LABOSI) and $Al(NO_3)_3.9H_2O$ (PROLABO) was added slowly under vigorous stirring into NaOH (2 M) and Na_2CO_3 (1 M) aqueous solution. The final pH was 9.5 and the resulting slurry was heated at 60 °C for 24 hours. Then, the precipitate was filtered, washed several times with hot deionized water (50 °C) and dried at 55 °C for 64 hours. Four samples were synthesized with different Co and Mg contents:

$Co_{6-x}Mg_xAl_2HT$ with x =0, 2, 4, and 6. Conventional Co_6Al_2OH sample was also prepared by co-precipitation of nitrate elements with NaOH. The final pH was 9.5 and the precipitate was directly filtered, washed several times with hot deionized water and dried at 100 °C for 24 hours. The calcination treatment was performed under flow of air (4 L/h, −2 °C/min, 4 hours at 500 °C); the solids obtained were named $Co_{6-x}Mg_xAl_2HT500$ (x = 0, 2, 4, 6), and Co_6Al_2OH500. The symbol HT is used to indicate samples synthesized from hydrotalcite preparation and the symbol OH is used to name the samples prepared from the classical synthesis.

2.2. Characterization of hydrotalcites, hydroxides and corresponding calcined samples

The specific surface areas of solids were determined by the BET method using a Quantasorb Junior apparatus, and the gas adsorbed at −196 °C was pure nitrogen.

The structure of solids was analyzed at room temperature by X-Ray Diffraction (XRD) technique in a Bruker D8 advance diffractometer equipped with a copper anode (λ = 1.5406 Å). The scattering intensities were measured over an angular range of $4^\circ < 2\theta < 80^\circ$ for all the samples with a step-size of $\Delta(2\theta) = 0.02^\circ$ and a count time of 6 s per step. The diffraction patterns have been indexed by comparison with the JCPDS files. Crystallite size was determined (Scherrer method) using a graphics based profile analysis program (TOPAS from Bruker AXS).

The activity of the catalysts (100 mg) was measured in a continuous flow system on a fixed bed reactor at atmospheric pressure. Before each test, the catalyst was reactivated in flowing air (2 L/h) at 500 °C for 4 hours. The flow of the reactant gases (100 mL/min with 1000 ppm of C_7H_8 and balance with air) was adjusted by a Calibrage CAL PC-5 apparatus constituted of a saturator and one mass flow controller. After reaching a stable flow, reactants passed through the catalyst bed and the temperature was increased from room temperature to 500 °C (1 °C/min). The feed and the reactor outflow gases were analyzed on line by a micro-gas chromatograph (VARIAN CP4900).

VOC products are sampled using sorbent tubes: Carbosieve III for light hydrocarbons (C_2–C_6) and Tenax for semi volatile hydrocarbons (C_7–C_{15}). The sampling is optimized by the use of two cartriges in series in order to check the breakthrough. After sampling, the cartridges are analyzed by the thermal desorption pre-concentration method, followed by a quantification by high resolution gas chromatography with flame ionization detector for compounds from C_2 to C_6 with a mass spectrometer detector for the compounds from C_7 to C_{15}. In the case of C_7 to C_{15}, the adsorbed substances are concentrated in a desorption chamber at 220 °C, before injection onto beginning of the cold column chromatograph (combi injector/desorption module – EM640 Brucker). Hydrocarbon identifications are assigned by comparing retention times of chromatographic peaks from emissions samples with those from standard mixtures and by comparing mass spectra with those contained in NIST and or WILEY libraries.

2.3. Cells and culture conditions

The cell line used originates from the normal lung tissue of a human embryo, and is deposited under the designation L132 in the American type culture collection (ATCC; ATCC number: CCL-5). The morphology of these cells is epithelial, and they exhibit typical features of pneumocytes. L132 cells were cultured in sterile plastic flasks (Corning; Thermo Fisher Scientific), in minimum essential medium with Earle's salts, containing: 5% (v/v) fetal bovine serum, 1% (v/v) L-glutamin (200 mM), 1% (v/v) penicillin (10,000 IU/mL), and 1% (v/v) streptomycin (10,000 UG/mL) (In Vitrogen-Life Technologies). Exponentially growing cells were maintained at 37 °C, in a humidified atmosphere containing 5% CO_2. All the L132 cells we used derived from the same initial cell culture [15].

2.4. Cytotoxicity of volatile organic compound

The cytotoxicity of the toluene and/or one of the by-products arising from its incomplete oxidative degradation, benzene, has been carried out in the human lung target L132 cell model using three complementary methods: the determination of LDH activity in cell-free culture supernatants (cytotoxicity detection kit LDH, Roche diagnostics), the determination of the MDH activity (cell proliferation reagent WST-1, Roche diagnostics) and the incorporation of BrdU (cell proliferation Elisa BrdU, Roche diagnostics) in cultured cells [16]. Briefly, to carry out the three methods, L132 cells were seeded in 96-well culture microplates (Costar; Thermo Fisher Scientific) at a density of 2×10^4 cells/200 μL culture media containing increasing concentrations of toluene (i.e. from 5000 to 80,000 ppm), benzene (i.e. from 5 à 80 ppm), or their association (i.e. benzene: 20 ppm; toluene: from 5000 to 80,000 ppm) and incubated at 37 °C in a humidified atmosphere containing 5% CO_2. Non-exposed cells were used as negative controls (i.e. 100% viability) and Triton X-100 (2%, v/v)-exposed cells as positive controls (i.e. 100% mortality). Accordingly, 16 replicates were chosen at random as negative control cells (i.e. 100% viability), eight replicates per VOC concentration as exposed cells, and eight replicates as positive controls (i.e. 100% mortality). After 6, 12, 24, 48 or 72 h of incubation, LDH activity in cell-free culture supernatants, on the one hand, and MDH activity and BrdU incorporation in cultured cells, on the other hand, were carried out.

2.5. Statistical analysis

Results are expressed as mean values and ranges (minimum value–maximum value). Data from cell cultures exposed to increasing concentrations of VOC were compared to those from non-exposed cell cultures. Statistical analyses were performed by the Mann-Whitney U test (software: SPSS for Windows, v10.05, 2000; Paris, France). Statistically significant differences were reported with p values < 0.05.

3. Results and discussion

3.1. Hydrotalcites and hydroxides precursors

The XRD patterns for all samples are shown in Fig. 1 and correspond to well crystallized layered materials. The peaks recorded are attributed to crystalline planes of a hydrotalcite structure (rombohedral 3R symmetry; JCPDS 220700). The unit cell parameter "a" is the average distance between two metal ions in the layers and "c" is three times the distance from the centre of one layer to the next. The parameter "a" has been calculated from the position of the first peak in the doublet close to $2\theta = 60^\circ$ given by plane (110) according to $a = 2 \times d$ (110). The "c" parameter has been calculated from the position of the peak close to $2\theta = 11^\circ$ given by plane (003) using the relationship $c = 3 \times d$ (003). The lattice parameters of the prepared HTs are listed in Table 1. For the same Mg/Al = 3 ratio, the "a" and "c" parameters are similar to those found by Lin et al. [17]. The Mg substitution by Co leads to a decrease of the "c" value. Nevertheless, Ribet et al. [18] have obtained an increase of the "c" value for hydrotalcites Co-Mg-Al ($(M^{2+}/Al^{3+}) = 2$). This result can be explained by the formation, of another phase containing cobalt which leads to an increase in the value of the $Al^{3+}/(Al^{3+} + M^{2+})$ ratio.

Indeed, it is accepted that the $Al^{3+}/(Al^{3+} + M^{2+})$ ratio increase leads to the decrease of the "c" parameter. This phenomenon is due to an electrostatic attraction increase between the positive charges in the brucite layer and the interlayer negative charges leading to OH-O bond length modification [18,19]. The "a" values (Table 1) are in agreement with those reported in the literature [20]. This is partly due to the Mg^{2+} substitution by a larger cation Co^{2+} ($rCo^{2+} = 0.74$ Å $> rMg^{2+} = 0.65$ Å) [20], and suggests the formation of a single phase hydrotalcite type. However, for samples with high cobalt content ($Co_4Mg_2Al_2HT$ and Co_6Al_2HT), a second phase (nitrate cobalt hydroxide JCPDS no. 460,605) is detected by the presence of a low diffraction peak at $2\theta = 33.7^\circ$. The XRD pattern of Co_6Al_2OH (not shown here) corresponds to $Co_5(O_{9.48}H_{8.52})NO_3$ compound (JCPDS 460,605) and hydrotalcite phase is not detected.

The XRD pattern of Co_6Al_2OH (not shown here) corresponds to $Co_5(O_{9.48}H_{8.52})NO_3$. The dried solids were characterized by nitrogen adsorption and the specific surface areas were calculated using the BET method (Table 1).

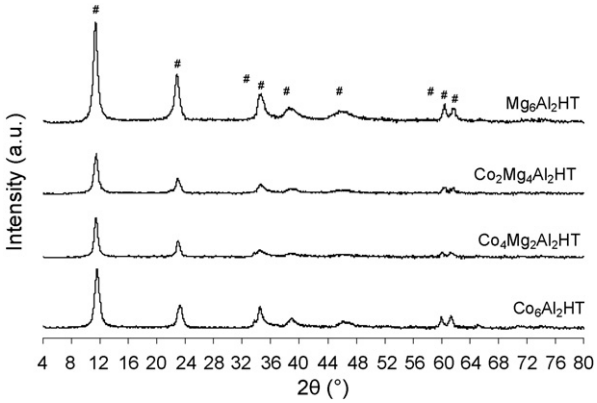

Fig. 1. XRD patterns of $Co_{6-x}Mg_xAl_2HT$ dried samples (#: hydrotalcite).

The specific area increases when Co replaces partially Mg and the value is the highest when Mg is totally substituted by Mg.

3.2. Characterization of calcined Co-Mg-Al hydrotalcites and hydroxides

The specific area (S_{BET}) and average pore diameter of the solids are presented in Table 1 (T = 500 °C). The N_2 adsorption–desorption isotherms are of type IV for all the synthesized samples, typical of mesoporous materials. The calcination at 500 °C of "HT" samples leads to an enhancement of specific area values (Table 1). This increase is more pronounced for the $Co_2Mg_4Al_2HT500$ sample. For the "OH" samples, the treatment at 500 °C provides to a significant decrease of specific area values. These different behaviours can be explained by the initial presence of the hydrotalcite phase. Reichle et al. [21] have attributed earlier that phenomenon to the pores/craters formation on the surface of the material through which water molecules and CO_2 escape (from interlayer) and showed that 60% of the specific area is due to the contribution of these pores. That phenomenon explains the porosity and the high specific area of our samples.

The XRD patterns of Mg_6Al_2HT500 and $Co_{6-x}Mg_xAl_2HT500$ are presented in Fig. 2. For both higher cobalt content solids, $Co_4Mg_2Al_2HT500$ and Co_6Al_2HT500, different diffraction peaks can be attributed to those of a spinel-type structure. The broadness of diffraction peaks can be also explained by the presence of a mixture of three oxide spinel phases very difficult to differentiate by XRD [20]: Co_3O_4 (JCPDS 421467), $CoAl_2O_4$ (JCPDS 440160) and

Table 1
XRD parameters, specific areas values and pores distributions.

Samples	Lattice parameters (Å)		Half width of (003) XRD peak (2θ en°)	Specific area (m^2/g)	Specific area (m^2/g)	Pores distributions (nm)
	c	a		T = 130 °C	T = 500 °C	T = 500 °C
Co_6Al_2HT	22.8759	3.0805	0.77	111	121	6–8
$Co_4Mg_2Al_2HT$	23.170	3.0744	0.57	80	72	11–14
$Co_2Mg_4Al_2HT$	23.133	3.063	0.68	88	208	4–6
Mg_6Al_2HT	77	3.0596	0.66	77	214	–
Co_6Al_2OH	–	–	–	141	53	–

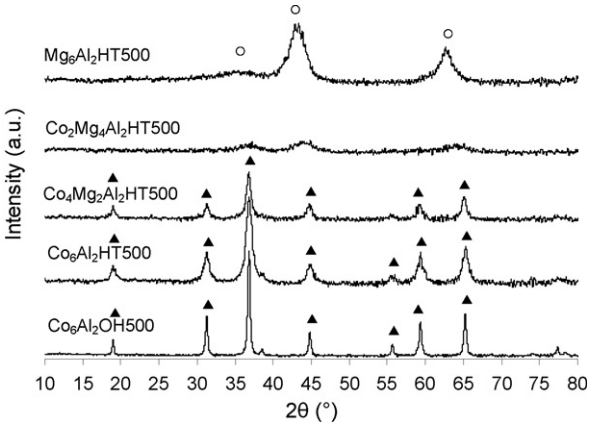

Fig. 2. XRD patterns of calcined $Co_{6-x}Mg_xAl_2HT500$ (o: MgO; ▲: Spinel).

Co_2AlO_4 (JCPDS 380814). The formation of Co_3O_4 is due to the easy oxidizability of Co^{2+} ions and the thermodynamical stability of Co_3O_4 (than CoO) in air [22].

For Mg_6Al_2HT500 sample, the XRD pattern reveals the formation of mixed oxides which are actually $Mg(Al^{3+})O$ solid solutions of MgO-periclase type because 2θ values are shifted towards highest 2θ values compared to the observed JCPDS no. 450,946 data. That shift could be explained by the substitution of a few Mg^{2+} ions by Al^{3+} ions (0.65 to 0.50 Å) [23]. The samples calcined at 500 °C are tested as catalysts in the toluene total oxidation (Fig. 3). When the toluene conversion is complete, H_2O and CO_2 are the only compounds observed. But before the total conversion, few ppm of hydrocarbons are detected. MgAlHT500 sample presents a weak activity in toluene oxidation with 10% of toluene conversion at 400 °C. Thus, the use of cobalt has a beneficial effect on the activity. The T_{50} temperature, at which 50% toluene conversion is achieved, is used to compare the catalytic activity of the

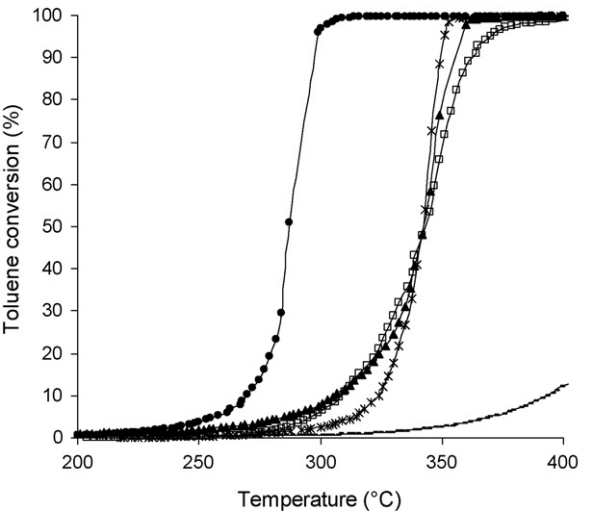

Fig. 3. Conversion of toluene (%) on $Co_{6-x}Mg_xAl_2HT500$ and Co_6Al_2OH500 catalysts vs reaction temperature (°C) (●: Co_6Al_2HT500; □: $Co_4Mg_2Al_2HT500$; x: $Co_2Mg_4Al_2HT500$; ▲: Co_6Al_2OH500; –: Mg_6Al_2HT500).

mixed oxides. The catalytic activity following order can be established:

$Co_6Al_2HT500 > Co_2Mg_4Al_2HT500 = Co_4Mg_2Al_2HT500 = C\text{-}Co_6Al_2OH500 >> Mg_6Al_2HT500$.

Correlations between the T_{50} values, the specific areas and the mixed oxides composition are observed. Indeed some results will be published in another paper. The amount of cobalt in the sample is one of the key factors for a high activity. However, $Co_2Mg_4Al_2HT500$ and $Co_4Mg_2Al_2HT500$ have close T_{50} values. The specific area of $Co_2Mg_4Al_2HT500$ (more than twice higher) could partly compensate the lower cobalt content (half the value) compared to $Co_4Mg_2Al_2HT500$.

Moreover, the $Co_6Al_2HT(500)$ sample is more active in the toluene oxidation than the same catalyst which is not synthesized via hydrotalcite phase. These catalytic results are in straight line with the highest specific area values obtained for "HT" calcined samples (Table 1).

The selectivity of the catalysts is evaluated through the identification and quantification of products. At 100% conversion, the selectivity in carbon products is totally for CO_2 (a carbon balance study has proved that result). But for a lower conversion of toluene, incomplete intermediate products are observed including a few ppm of benzene. In the oxidation of toluene, different reaction pathways have already been identified [24]. The first and the most important reaction path is the one initiated by attack of the methyl group with subsequent oxidation step. The second path is also initiated by attack on the methyl group but subsequent oxidative coupling forming dimers that are oxidized further. The third reaction path is due to the direct oxidation in the aromatic nucleus and occurs to a very low extent [24].

The identification of these products was conducted during the catalytic activity of the Co_6Al_2HT500 catalyst. During the test, for an incomplete conversion of toluene, the emergence of secondary products was discovered. According to the literature, the oxidation of toluene in the presence of a catalyst could lead to the different products formation. During the test, we also conducted a sampling of the gases emerging from the test catalytic reactor. The sampling was carried out by gas adsorption on a cartridge with adsorbent. The adsorbed gas can be extracted by thermal desorption. The sampling is conducted in the following sequence: the cartridges are mounted in series output reactor test to trap carbon organics products. The duration of sampling is conducted under a gas flow of 100 mL/min for 15 min in the temperature 286-300 °C range. The cartridges are thermodesorbed by heating for 1.5 min at 220 °C and the desorbed gases were analyzed by GC-MS. The organic products trapped on the cartridges are: benzene, styrene, benzoquinone, benzaldehyde, benzofurane, acetophenone, naphthalene, biphenyl, furan and benzyl alcohol. The presence of three by-products can be explained by the selective oxidation of toluene [25] and the different parallel reaction paths describes by Lars et Andersson [24].

Fig. 4 shows spectra after operando DRIFT of Co_6Al_2HT500 during VOC total oxidation. This study allows us to follow toluene oxidation and its adsorption. The band due to C-H aliphatic stretching at 3060/cm which is visible

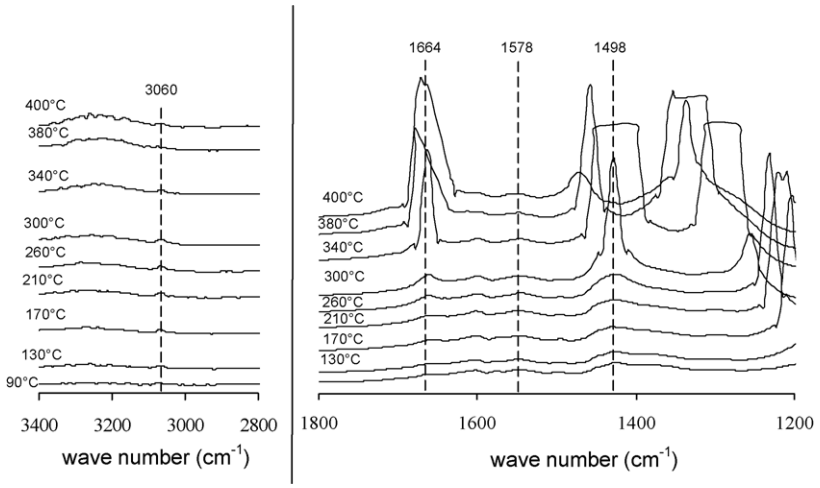

Fig. 4. Operando DRIFT over Co_6Al_2HT500.

until 360 °C can relate to vibration of the C-H radical of the exocyclic methyl. The bands observed at 1498 and 1578/cm are ascribed to the vibration of the aromatic nucleus C = C bonds; the first one is visible up to 320 °C whereas the second up to 230 °C. According to the toluene light-off curve, this latter corresponds to the temperature for which the conversion begins and the last one at 320 °C coincides to the minimum temperature for toluene total oxidation. At higher temperature, up to 400 °C, bands at 1604 and 1707/cm are detected. The first can be related to the vibration of C = C bonds from aromatic compounds which belongs to toluene highly adsorbed on the catalyst and their oxidation occurs at higher temperature. The second at 1707/cm is attributed to substituted-aromatic due to coke formation. Moreover three bands at 1664, 1427 and 1540/cm are detected; those are characteristic of carbonated compounds. The first band whose intensity increases with temperature is attributed to hydrogenocarbonates, the second one to polydentate carbonates and the third to monodentate carbonates.

These attributions are previously confirmed by a DRIFT study of the sample in the presence of 10,000 ppm of CO_2 diluted in air.

In addition, at the end of the catalytic test, the sample was cooled at room temperature and then heated under nitrogen flow to analyze by GC-MS the composition of the effluent stream. The desorbed compounds observed are then styrene, benzaldehyde and traces of acetophenone. This result confirms operando DRIFT study and illustrates the complexity of aromatic compounds oxidation.

3.3. Study of the cytotoxicity of volatile organic compound

The cytotoxicity of the toluene and/or one of the by-products arising from its incomplete oxidative degradation, benzene, have been carried out in L132 human lung target cell model using three complementary methods: the determination of LDH activity in cell-free culture supernatants, and the determination of the MDH activity and the incorporation of BrdU in cells (Fig. 5).

With regards to the exposure of L132 cells to increasing concentrations of toluene, statistically significant increases of extracellular LDH activity were observed in cell culture supernatants 24 h or 48 h after L132 cell exposure to toluene at concentrations greater or equal to 10,000 ppm, versus controls ($p < 0.01$). Such increases of extracellular LDH activity in cell-free culture supernatants only 24 h or 48 h after L132 cell exposure to toluene indicate the occurrence of alterations of cell membrane integrity and/or permeability, leading thereby to the liberation of the LDH enzyme from the intracellular compartment (i.e. cytoplasm) to the extracellular compartment (i.e. cell culture supernatant) [26]. The cell membrane is the biological membrane separating the interior of a cell from the outside environment. It is a semi-permeable lipid bilayer found in all cells. It contains a wide variety of biological molecules, primarily proteins and lipids, which are involved in a vast array of cellular processes such as cell adhesion, ion channel conductance and cell signaling [27].

Moreover, as shown by Fig. 5, MDH activities in toluene exposed L132 cells significantly decreased only 72 h after their exposure to toluene concentrations greater or equal to 5000 ppm, versus controls ($p < 0.01$), suggesting thereby the alteration of mitochondrial metabolism, a key organelle of cell. Accordingly, the determination of MDH activity reflects in fact both the cell toxicity and the cell proliferation, since it depends on the amount as well as the mitochondrial metabolic competence of cells. In cell cytoplasm, mitochondria are membrane-enclosed organelles found in most eukaryotic cells [28]. Mitochondria are sometimes described as "cellular power plants" because they generate most of the cell's supply of adenosine triphosphate used as a source of chemical energy [29]. In addition to supplying cellular energy, mitochondria are involved in a range of other processes, such as signaling, cellular differentiation, cell death, as well as the control of the cell cycle and cell growth [30].

In contrast, whatever the considered incubation time, no significant alteration of BrdU incorporation in toluene-

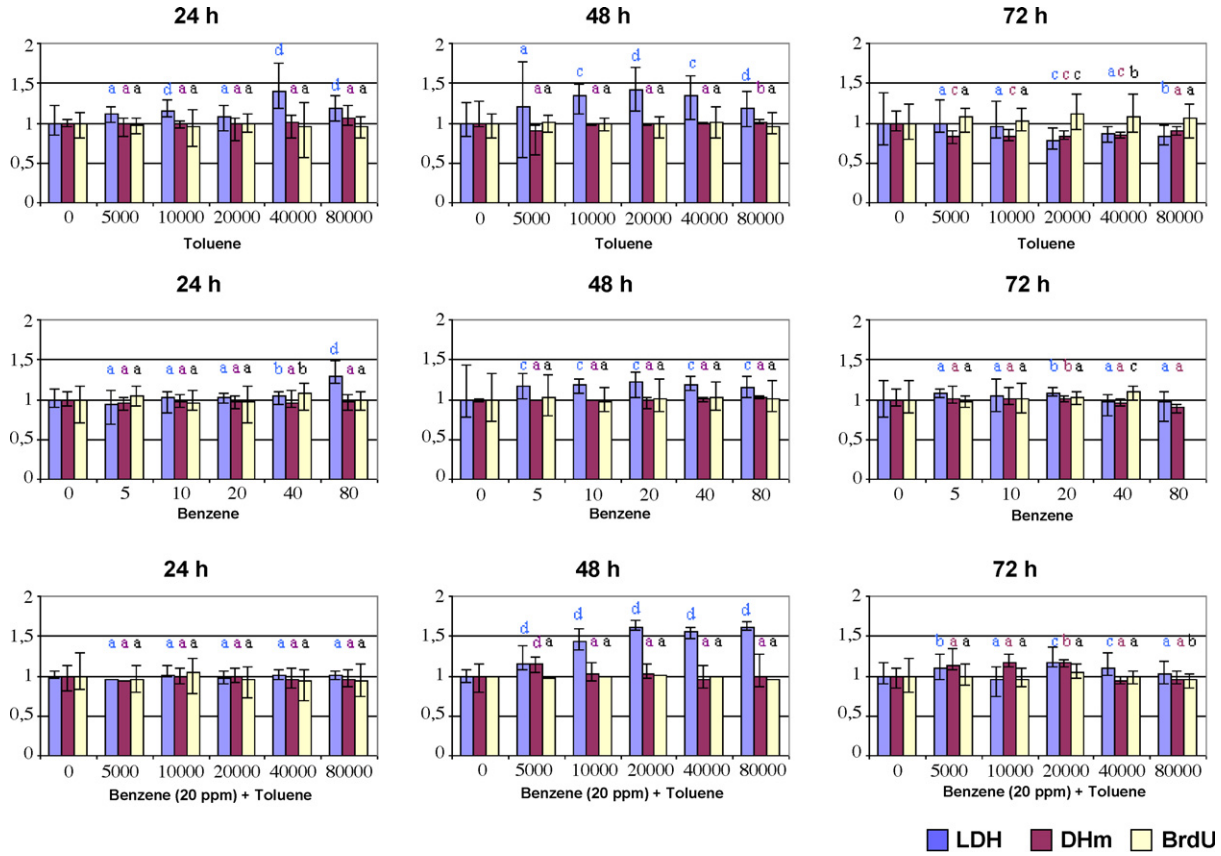

Fig. 5. Determination of the lactate dehydrogenase (LDH) activity (% vs controls) in L132 cell-free culture supernatants, and mitochondrial dehydrogenase (MDH) activity (% vs controls) and incorporation of 5-Bromo-2-deoxyuridine (BrdU) (% vs controls) in L132 cells, 24, 48 or 72 h after the incubation of L132 cells in the continuous presence of increasing concentrations of toluene (i.e. from 5000 to 80,000 ppm), benzene (i.e. from 5 à 80 ppm), or their association (i.e. benzene: 20 ppm; toluene: from 5000 to 80,000 ppm) without renewing the culture media. Non-exposed cells were used as negative controls (i.e. 100 viability). These values are depicted as mean values and standard deviations of 16 replicates for negative controls (i.e. 100% viability) and eight replicates for every volatile organic compound concentrations (Mann-Whitney U test; vs controls; a: not significant; b: $p < 0.05$; c: $p < 0.01$; d: $p < 0.001$).

exposed L132 cells was reported, indicating thereby no alteration of cell proliferation and/or DNA synthesis. Indeed, as BrdU is a synthetic nucleoside that is an analogue of thymidine, it is commonly used in the detection of proliferating cells in living tissues, through the determination of DNA synthesis. BrdU can be incorporated into the newly synthesized DNA of replicating cells (during the S phase of the cell cycle), substituting for thymidine during DNA replication [17].

Taken together, these results allow us to conclude that, in the L132 human lung target cell model we used, the exposure to toluene induced alteration of both the cell membrane integrity and/or permeability (after 24 and 48 h) and the mitochondrial metabolism (only after 72 h).

In view of the results arising from benzene-exposed L132 cells, statistically significant increases of extracellular LDH activities in L132 cell culture supernatants were observed 24 h after L132 cell exposure to benzene at concentrations greater or equal to 40 ppm, and 48 h after their exposure to benzene at concentrations greater or equal to 5 ppm, versus controls ($p < 0.05$). Such data support the occurrence of a significant alteration of the cell membrane integrity and/or permeability in the L132 human lung target cell model we used, in response to benzene exposure, even at relatively low concentrations (i.e. 5 ppm). However, whatever the considered incubation time, Fig. 5 shows that neither MDH activities nor BrdU incorporation were significantly changed in benzene-exposed L132 cells, versus controls, indicating thereby that, in the L132 human lung target cell model we used, benzene, at the concentrations we tested and the considered endpoints we observed, did to alter mitochondrial metabolism, cell proliferation, and/or DNA synthesis.

At least, Fig. 5 shows that there were statistically significant increases of extracellular LDH activities in L132 cell culture supernatants 24 h or 48 h after L132 cell exposure to benzene (i.e. 20 ppm) and toluene (i.e. greater or equal to 5 ppm), versus controls ($p < 0.01$). It is important to highlight that such increases in extracellular LDH activities in L132 cell culture supernatants from L132 cell exposed to the associations between toluene and benzene were higher than those from L132 cells exposed to either toluene or benzene. The association between the two VOC also induces severe alterations of the cell membrane integrity and/or permeability, but does not

lead to significant alterations of mitochondrial metabolism, cell proliferation, and/or DNA synthesis.

4. Conclusion

In this study, Co-Mg–Al hydrotalcites with different compositions were prepared by a coprecipitation method. The thermal decomposition at 500 °C led to mixed Co-Mg oxides with high specific areas (around 100 m^2/g). Higher activity for toluene oxidation was observed in the presence of Co rich samples especially for $Co_6Al_2HT(500)$. It is important to note that the activity was increased when the sample Co_6Al_2 was prepared through hydrotalcite precursor. This result may be explained by the greater specific area and well dispersed oxides. In addition, the amount of benzene formed in the oxidation of toluene was more important for the compound prepared by conventional synthesis compared to that obtained though hydrotalcite pathway. The "operando" DRIFT and GC-MS analysis allowed us to identify the intermediate oxidation products.

Concerning the results arising from the cytotoxicity study of toluene and/or benzene, the L132 human lung target cell model, we used allowed us to conclude that not only the exposure to toluene or benzene but also the exposure to their association induced alteration of cell membrane integrity and/or permeability. With other respects, this indicates that in the case of an incomplete catalysis, driven by non-optimal conditions (e.g. temperature) or by inactivation of the catalyst (e.g. aging, poisoning), toxic by-products formed during the catalysis treatment (i.e. benzene) may interact with the initial VOC (i.e. toluene) to cause high cell alterations.

Conflicts of Interest

The authors have no conflict of interest.

Acknowledgment

This work was supported by the "Région Nord – pas de Calais" through a research grant. The authors thank also the European community through an Interreg IV France-Wallonie-Flandre project ("Redugaz") and Walloon Region for financial supports.

References

[1] A. O'Malley, B.K. Hodnett, Catal. Today 54 (1999) 31.
[2] S.H. Taylor, C.S. Henegan, G.J. Hutchings, I.D. Hudson, Catal. Today 59 (2000) 219.
[3] M. Baldi, E. Finocchio, F. Milella, G. Busca, Appl. Catal. B. Env 16 (1998) 43.
[4] T. Ataloglou, J. Vakros, K. Bourikas, C. Fountzoula, C. Kordulis, A. Lycourghiotis, Appl. Catal. B. Env 57 (2005) 299.
[5] F. Cavani, F. Trifiro, A. Vaccari, Catal. Today 11 (1991) 173.
[6] A. Vaccari, Appl. Clay Sci 14 (1999) 161.
[7] S.T. Yong, K. Hidajat, S. Kawi, J. Power Sources 91 (2004) 131.
[8] K. Takehira, T. Shishido, D. Shoro, K. Murakami, M. Honda, T. Kawabata, K. Takaki, Catal. Commun 5 (2004) 209.
[9] A. Alejandre, F. Medina, X. Rodriguez, P. Salagre, J.E. Sueiras, J. Catal 188 (1999) 311.
[10] J.F. Lamonier, A.B. Boutoundou, C. Gennequin, M.J. Perez Zurita, S. Siffert, A. Aboukais, Catal. Letters 118 (2007) 165.
[11] R. Zhao, C. Yin, H. Zhao, C. Lin, Synthesis, Fuel Proces. Technol 81 (2003) 201.
[12] S. Kannan, Appl. Clay Sci 13 (1998) 347.
[13] A.E. Palomares, J.M. Lopez-Nieto, F.J. Lazaro, A. Lopez, A. Corma, Appl. Catal. B. Env 20 (1999) 257.
[14] C. Gennequin, R. Cousin, J.-F. Lamonier, S. Siffert, A. Aboukais, Catal. Com 9 (2008) 1639.
[15] G. Garcon, Z. Dagher, F. Zerimech, F. Ledoux, D. Courcot, A. Aboukais, E. Puskaric, P. Shirali, Toxicol. In Vitro 20 (2006) 519.
[16] S. Billet, G. Garcon, Z. Dagher, A. Verdin, F. Ledoux, F. Cazier, D. Courcot, A. Aboukais, P. Shirali, Environ. Res 105 (2007) 223.
[17] Y.J. Lin, D.Q. Li, D.G. Evans, X. Duan, Polymer Degrad. Stab 88 (2005) 296.
[18] S. Ribet, D. Tichit, B. Coq, B. Ducourant, F. Morato, J. Solid State Chem 142 (1999) 382.
[19] G. Brown, M.C. Gastuche, Clay Miner 7 (1967) 177.
[20] J. Pérez-Ramirez, G. Mul, F. Kapteijn, J.A. Moulijn, Mat. Res. Bull. 36 (2001) 1769.
[21] W.T. Reichle, S.Y. Kang, D.S. Everhardt, J. Catal 101 (1986) 352.
[22] T. Sato, U. Fujita, T. Endo, M. Shimada, A. Tsunashima, Reac. Solids 5 (1988) 219.
[23] M.J. Hernandez Moreno, M.A. Ulibarri, J.L. Rendon, C.J. Serna, Phys. Chem. Minerals 12 (1985) 34.
[24] S. Lars, T. Andersson, J. Catal 98 (1986) 138.
[25] G. Centi, P. Lanzafame, S. Perathoner, Catal. Today 99 (2005) 161.
[26] A. Baulig, J.J. Poirault, P. Ausset, R. Schins, T. Shi, D. Baralle, P. Dorlhene, M. Meyer, R. Lefevre, A. Baeza-Squiban, F.F Marano, Environ. Sci Technol 38 (2004) 5985.
[27] S.J. Singer, G.L. Nicolson, Science 175 (23) (1992) 720.
[28] K. Henze, W. Martin, Nature 426 (2003) 127.
[29] B. Campbell, A. Neil, B. Williamson, R.J. Heyden Boston, Massachusetts: Pearson Prentice Hall. (2006) ISBN 0-13-250882-6.
[30] H.M. Bride, M. Neuspiel, S. Wasiak, Curr. Biol 16 (2006) R551.